

# Comprehensive Study on Cr(VI) Adsorption and Regeneration Behavior of Alkali-Treated Wood Charcoal: Isotherms and Kinetics Models



Moh. Azhar Afandy<sup>a,\*</sup>, Fikrah Dian Indrawati Sawali<sup>a</sup>

<sup>a</sup>Mineral Chemical Engineering, Politeknik Industri Logam Morowali, Morowali, 94974, Indonesia Corresponding author: azhar@pilm.ac.id

#### **Abstract**

The present study considers the adsorption and regeneration behavior of alkali-treated wood charcoal (WC-NaOH and WC-KOH) for Cr(VI) removal. Adsorption isotherms (Langmuir, Freundlich, Temkin, and Dubinin-Raduskevich) and kinetics (Pseudo-first-order and Pseudo-second-order being investigated utilizing a non-linear method that provides precise parameter prediction and mechanism elucidation. The outcomes suggested that both WC-NaOH and WC-KOH exhibit good Cr(VI) removal efficiency, with the Langmuir model best explaining the adsorption phase, indicating single-layer adsorption. The kinetic study revealed that the Pseudo-second-order model aligns remarkably well with the data, thereby affirming that chemical adsorption is the predominant mechanism in consideration. A comparative analysis revealed that WC-KOH exhibits a higher amount of adsorption than WC-NaOH, attributable to its enhanced larger surface area as well as micro-porous structure. Regeneration studies showed the possibility of reuse of both adsorbents. It shows the efficiency of alkali-treated wood charcoal for Cr(VI) decontamination and the advantages of non-linear modelling in adsorption experiments.

Keywords: Adsorption; Chromium; Isotherm; Kinetics; Wood charcoal

#### 1. Introduction

The demand for renewable natural resources is growing globally, and the production of charcoal from biomass is a promising approach [1], [2], [3]. Charcoal has diverse applications, includes application as an adsorption material to obtain the elimination of toxic metals such as chromium from polluted water [1]. Biochar, another type of charcoal, has been extensively explored for its potential for the sanitation and water treatment based on its extensive surface area, porous structure, or functional groups [2], [4], [5]. However, the establishment alongside the optimization of biocharbased processes remain largely unknown [6]. Chromium, particularly the chromium hexavalent (Cr(VI)), is a toxic heavy metal that requires efficient removal from industrial effluents. The toxicity of chromium can be mitigated by converting it to the less toxic trivalent form through adsorption on a suitable adsorbent[7], [8], [9]. Pollution of water resources by hexavalent chromium (Cr(VI)) is an important worldwide concern related to its severe environmental impact, carcinogenic qualities, and extensive use in numerous industries such as metal plating, leather tanning, and dye manufacture. Cr(VI) represents a serious hazard for the well-being of humans and also environments, hence effective technologies are needed to remove it from wastewater [10], [11], [12], [13], [14], [15].

Although the usefulness of wood charcoal as an adsorbent has been known, its performance for Cr(VI) removal has not been completely examined in terms of adsorption isotherm, kinetics, and regeneration ability. Most investigations have focused on raw or barely treated adsorbents, leaving a gap in understanding regarding the influence of chemical activation employing alkali (such as NaOH and KOH) on adsorption performance. In addition, many research still employe linearization models for isotherm and kinetics analysis, which can result in parameter estimation mistakes and limit the knowledge of the adsorption mechanism and capacity. Several earlier investigations, such as those conducted by Khandelwal,2020; Sahin, 2015; Markandeya, 2015; and Umar, 2017; [16], [17], [18], [19] demonstrated that the non-linear model had a greater estimation of parameters precision since this model directly reduces the disparity between observed and predicted outcomes without conducting mathematical manipulations that

can skew the results. In addition, the non-linear model reduces statistical mistakes related to linearization. The non-linear modeling approach is also crucial to depict the adsorption behavior more precisely and to estimate key parameters such as the maximum adsorption capacity (qmax) and rate constant[20], [21].

The lack of comprehensive studies comparing the adsorption behavior of activated wood charcoal with different chemicals (NaOH and KOH) generates a substantial knowledge gap. Furthermore, the regeneration capability of this material, which is a key component for practical applications, is still infrequently addressed. Recent investigations have proven the potential of biomass-based materials for Cr(VI) adsorption, with chemically treated adsorbents demonstrating higher performance due to an elevated surface region, permeability, as well as the existence of active functional areas. However, evidence on the comparative effectiveness of WC-NaOH and WC-KOH in adsorption and regeneration under real wastewater conditions is still scarce. Given the abundance of agricultural waste in countries with strong industrial activity, such as Indonesia, the practical application of wood residue as an initial component for adsorbents is in conformity with local sustainability goals and resource availability.

In the current research, we explore the equilibrium adsorption isotherms, kinetics, and regeneration studies to elimination Cr(VI) coming from water-based solutions utilizing alkali-treated wood charcoal as the adsorbent. Several isotherms, including Langmuir, Freundlich, Temkin, and Dubinin-Raduskevich models, used for defining the equilibrium adsorption data, and the kinetics were examined using pseudo-first-order and pseudo-second-order models. The influence of beginning concentration, quantity of adsorbent, and adsorption time on Cr(VI) removal were also examined to optimize the process. This study also implemented an adsorbent regeneration approach to improve the adsorbent's lifespan of use, sustain efficiency, and promote sustainability through the reuse of existing components. This study utilized nonlinear kinetic and isotherm models to provide more precise parameter estimates than linear models and also to more effectively explain adsorption behavior. This approach is also more adaptable in controlling data that changes under different operating parameters, both at low or high concentrations. The results of the current study aim to bridge the existing research gap by offering an in-depth explanation of the adsorption mechanism, highlighting the function of alkali activation, and providing insights into the actual use of this material in Cr(VI) wastewater treatment.

# 2. Materials and Methods

# 2.1 Chemicals

Potassium dichromate (K<sub>2</sub>Cr<sub>2</sub>O<sub>7</sub>) is mixed in purified water to make a mixture of synthetic waste water, which will be used in the batch adsorption process. Potassium hydroxide (KOH) and sodium hydroxide (NaOH) were has been used to be chemical activators. Diphenyl carbazide, acetone, and H<sub>2</sub>SO<sub>4</sub> were utilized in the determination of Cr(VI) in the samples. Ethanol 95% is used in regeneration studies. All materials utilized in this research were sourced from local suppliers with specifications of analytical grade with 99% purity.

# 2.2 Adsorbent Preparation

Wood charcoal (WC) is obtained in the Bahodopi, Morowali, Indonesia area and is circulating on the market. The WC was crushed with a grinder followed by separated to smaller particles of 100 mesh and dried in the oven (Cryste) for 2 hours at 110° C. After that, the activation procedure was carried out using two types of chemical activators: KOH, and NaOH to see the impact of the activator type on the adsorption capacity of WC adsorbent. A chemical activation process was performed by employing 250 g of WC adsorbent for each,then adding 1 L of 0.1 M NaOH, and 0.1 M KOH for 3 hours, at a speed of 200 rpm. Next, the WC adsorbent that has been activated is separated by applying filtration paper and also rinsed with purified water until it reaches pH 7. The adsorbent that has been obtained is then re-dried in the oven for 2 hours at 110°C. Carbonization process continues at 650°C for 2 hours in the Muffle furnace (*Nabertherm b180*), following which the adsorbent is prepared for utilization.

# 2.3 Batch Adsorption Experiments

Batch study of adsorption have been performed employing WC adsorbent, and then putting it in an erlenmeyer flask holding 50 mL of adsorbate, and stirring at 200 rpm. After a while, the solution then filtered using to distinct filtrates and residue. The filtered solution generated was subsequently investigated using UV-Vis spectrophotometry (ICEN 350 - 1020) at a wavelength of 540 nm using standard methods (SNI 6989.71:2009). This batch adsorption

investigation took place to see its effect of Cr (VI) concentration (10-200 mg/L) adsorption time (0-120 min) alongside adsorbent dossage (0.5-1.5 g). This experiment was conducted out at room temperature (±28°C). The capacity of adsorption of Cr (VI) is able to obtained with the following equation:

$$q_e = \left\lceil \frac{\left(C_O - C_e\right) \times V}{m} \right\rceil \tag{1}$$

Where Co and Ce are the initial concentration values, that result concentration of Cr (VI) (mg/L) in the solution, qe is the amount of Cr(VI) adsorbed (mg/g), V is the volume of solution (L), and m is the mass of the WC adsorbent.

#### 2.4 Adsorption Isotherm

This experiment uses a form of non-linear adsorption isotherm. This model has more complicated computations compared to the linear isotherm model but may produce more accurate experimental results. In this experiment, multiple adsorption isotherm models were utilized, including the Langmuir, Freundlich, Temkin, Dubikinin-Radushkevich [22], [23], [24]. The equations for each model can be viewed in Table 1.

**Isotherm Models Equation**  $q_e = \frac{q_m K_L C_e}{1 + K_I C_o}$ Langmuir  $q_e = K_F C_e^{\frac{1}{n}}$ Freundlich  $q_e = \frac{RT}{B_T} \ln(A_T C_e)$ Temkin  $q_e = q_s \exp(-K_{DR}\varepsilon^2))$ **Dubinin-Raduskevich** 

Table 1. Non-linear form isotherm models.

#### 2.4 Adsorption Kinetics

Several model equations used to evaluate The kinetic variables that occur within the procedure for adsorption are able to seen in Table 2.

Table 2. Non-linear kinetics models

| <b>Kinetics Models</b> | Equation  |
|------------------------|---|
| Pseudo First Order     | $q_t = q_e(1 - \exp(-k_1 t))$                     |
| Pseudo Second<br>Order | $q_{t} = \frac{k_{2}q_{e}^{2}t}{1 + k_{2}q_{e}t}$ |

Where qt is the adsorption capacity (mg/g), qe is the adsorption capacity at equilibrium (mg/g), t is the adsorption time (minutes), k<sub>1</sub> is the pseudo-first order rate constant (/minute), k<sub>2</sub> is the pseudo-rate constant -second order (mg/mg.minute) [25], [26]. The isotherm model and kinetics of Cr(VI) adsorption by WC adsorbent can be evaluated using multiple error functions to figure out relationship between the model and experimental data. Coefficient of correlation ( $R^2$ ), sum square error (SSE), and chi square ( $x^2$ ). The smaller values of several of these parameters imply an ideal match of the isotherm alongside kinetic model findings and data from experiments. The Sum of Squared Errors (SSE) quantifies the total squared deviation between the observed adsorbate concentration values and those predicted by the model, a lower SSE indicates a superior model fit. Meanwhile, the chi-square (x<sup>2</sup>) value is used to quantify the variance between the experimental data and the model prediction outcomes by considering the data weight, where a lower x<sup>2</sup> value implies a greater prediction accuracy. The evaluation of the isotherm model not only rely on the R<sup>2</sup> value but also considers the SSE and x<sup>2</sup> values as crucial indicators to identify the model with the greatest prediction accuracy for Cr(VI) adsorption data by alkali-activated wood charcoal.

IPTEK, The Journal of Engineering, Vol. 11, No. 2, 2025 (eISSN: 2807-5064)

$$R^{2} = \frac{\sum_{i=1}^{n} (qt_{pred.} - \overline{qt_{exp.}})^{2}}{\sum_{i=1}^{n} (qt_{pred.} - \overline{qt_{exp.}})^{2} + \sum_{i=1}^{n} (qt_{pred.} - qt_{exp.})^{2}}$$
(2)

$$SSE = \sum_{i=1}^{n} \left( qt_{\text{exp.}} - qt_{\text{pred.}} \right)^{2}$$
 (3)

$$x^{2} = \sum_{i=1}^{n} \frac{(qt_{\text{exp.}} - qt_{pred.})^{2}}{qt_{pred.}}$$
(4)

# 2.5 Regeneration and Desorption Study

The steps of regeneration and desorption studies for the adsorption phase of Cr(VI) onto WC-NaOH and WC-KOH followed the previous approach conducted by Qu et al. [27] with modest alterations. We carried out the process in phases, finishing 4 cycles. Each experiment carried out the adsorption phase with a Cr(VI) concentration of 50 mg/L for 4 hours, followed by an analysis utilizing UV-Vis spectrophotometry. The residue obtained was then reused by dissolving it in a combination of ethanol and 0.1 M NaOH.

# 3. Results and Discussion

# 3.1 Effect of Initial Concentration

The initial concentration of Cr (VI) may exhibit an influence affecting the adsorption efficiency of the WC adsorbent. The efficiency value of the ion removal procedure on the concentration of Cr(VI) relies on the quantity of surface accessible on the adsorbent surface. So it is required to examine the performance of the WC adsorbent at varied Cr (VI) concentrations. The implications of Cr(VI) concentration for the adsorption capacity value of the WC adsorbent can be shown in Figure 1.

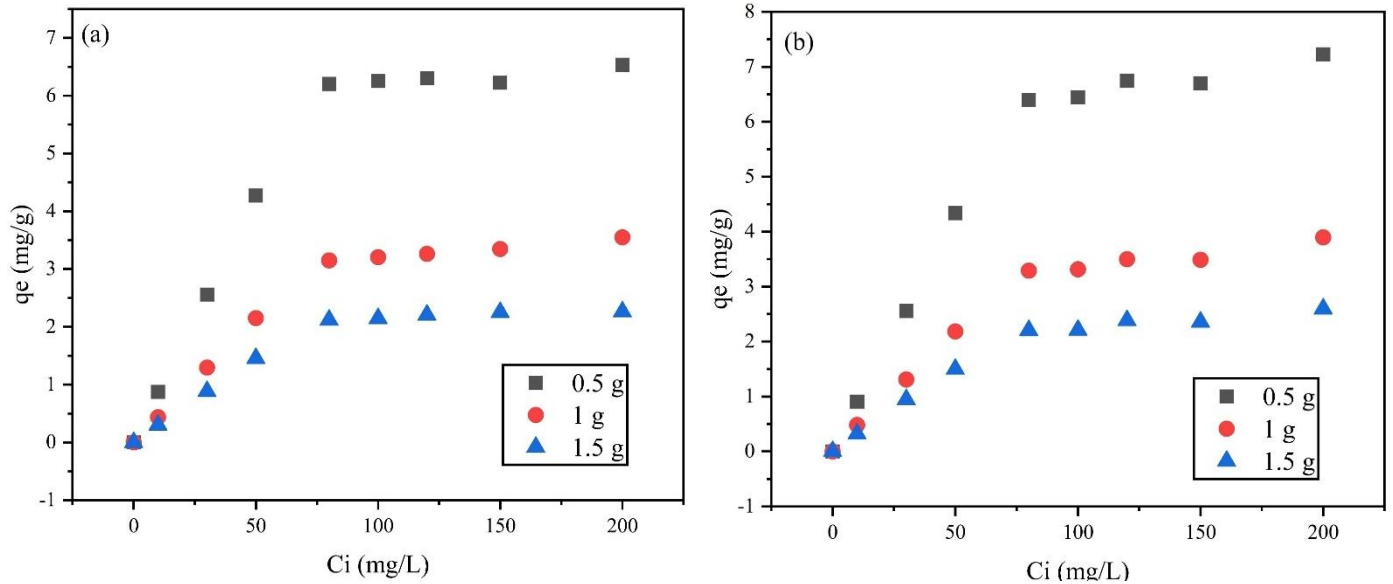


Figure 1. Effect of Initial Concentration for Cr(VI) removal (a) WC-NaOH, (b) WC-KOH

In Figure 1, we can observe how the adsorption capacity of the WC would rise collectively with the initial quantity of Cr (VI). This happens when a larger concentration of Cr (VI) will give an extra moving force to surpass the resistance in the solid-liquid mass transfer process. On the other hand, at concentrations that tend to be smaller, there will be many empty active sites that are not being utilized by Cr (VI) molecules, and this can be read as a decline in adsorption capacity. Increasing the concentration over the optimal level will result in an overall decrease in active sites on the outer surface of the adsorption medium consequently slowing down the mechanism of adsorption.

WC adsorbent activated by KOH gives much better adsorption capacity values as compared to NaOH. This is owing to the KOH activator tends to generate a greater amount of surface area compared to the NaOH activator, which tends to produce activated charcoal with a larger pore size. This is in keeping with studies done by Chia *et al* [28], which reveals that the surface area of activated carbon derived from the husk of rice with a KOH activator is larger than that employing a NaOH activator. This will subsequently trigger the creation of pores and pore volumes of activated carbon with a greater surface area. Apart from that, KOH has a greater degree of porosity when compared to NaOH, which happens owing to the activation of higher base cations in the alkali group, therefore KOH will create more base cations and can react better with carbon when compared to NaOH [29].

# 3.2 Effect of Contact Time

The period of contact is an essential element who may impact the step of adsorption. In principle, the more duration of the interaction periods, increased possibility offers for the adsorbate to make contact with the adsorbent, such that the adsorption capacity improves. However, beyond an optimal point, the adsorption capacity will approach a saturation point and no longer increase. Therefore, the ideal contact time must be chosen so that the greatest adsorption capacity may be reached. To explore the impacts of time on the Cr(VI) adsorption process employing WC adsorbent, this research was carried out in the time range of 20–120 minutes and can be shown in Figure 2.

Based on the results obtained in Figure 2, it suggests that the more time, it increases the adsorption capacity of the adsorbent. The adsorption process takes occur quite rapidly in the early moments since the availability of empty active sites on the surface of the adsorbent, and gradually diminishes as the available active sites decrease until equilibrium is achieved. The most favorable duration for interaction between Cr (VI) and the adsorbent in this investigation was shown to be 20 minutes. Upon adsorption of Cr(VI) onto the adsorbent sites, the quantity of active sites inside the adsorbent will diminish, thereby leading to a reduction in the rate of the adsorption process. The contact time in the adsorption process may be improved to decrease the quantity of adsorbent required and the duration of contact needed. The duration of adsorption also impacts the properties of the desorption process, as a longer contact time leads to a greater amount of desorbed material.

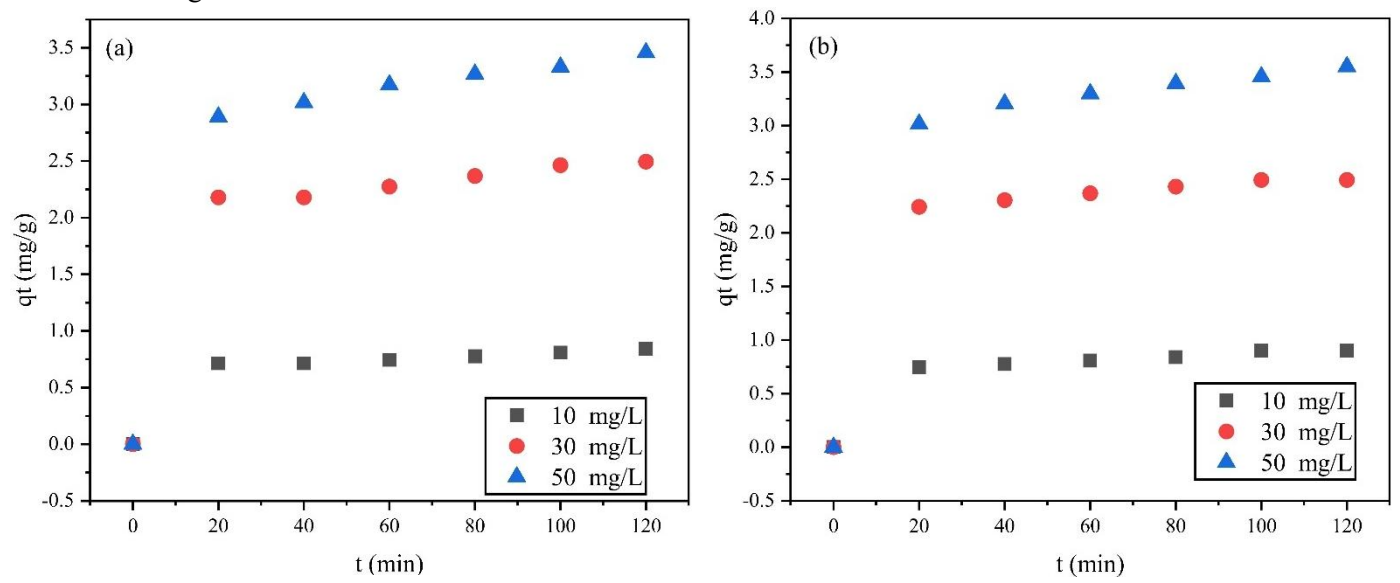


Figure 2. Effect of contact time for Cr(VI) removal (a) WC-NaOH, (b) WC-KOH

## 3.3 Langmuir Isotherm

The Langmuir isotherm model is able to utilized to presume that the procedure of adsorption takes place on a homogenous surface containing a limited amount of equivalent sites. The Langmuir isotherm approach proposes the the highest adsorption capacity of an adsorption medium is determined by a formation of a monolayer on the outermost layer, consisting of active locations which are directly correlated to the entire surface region. The adsorption process is restricted to a monolayer layer as each active site has the capacity to adsorb only one molecule. The Langmuir isotherm model derived from this study is seen in the Figure 3.

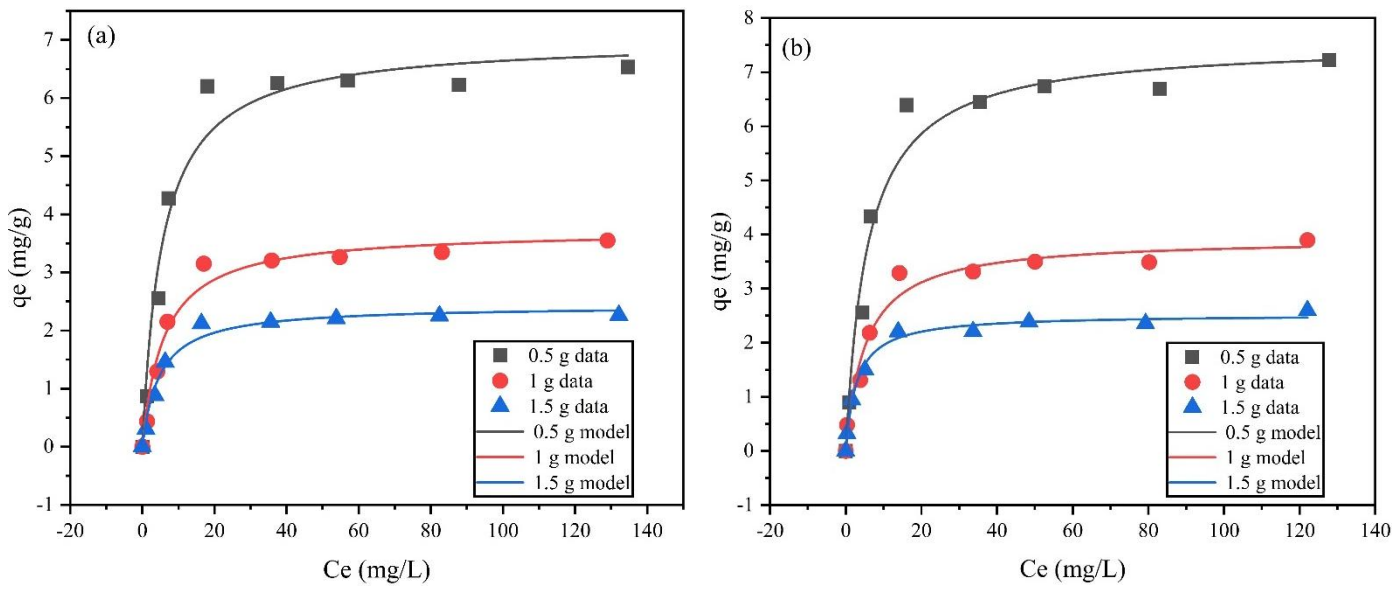


Figure 3. Langmuir isotherm model (a) WC-NaOH, (b) WC-KOH

Depending on the outcomes from Figure 3, the NaOH-WC offers the highest adsorption capacity (qmax) value of 1.4017 mg/g and the KOH-WC has a maximum adsorption capacity value of 1.5092 mg/g. Additionally, the  $K_L$  values for NaOH-WC and KOH-WC are 0.1806 L/mg and 0.1738 L/mg, respectively. A higher  $K_L$  value signifies a heightened affinity of the adsorbent for the adsorbate, indicating a more powerful interaction between the two. Based on the Langmuir isotherm model, it can be inferred that the NaOH-WC adsorbent has a higher affinity for binding Cr(VI) ions compared to the KOH-WC adsorbent. In addition, the dimensionless constant or separation factor  $(R_L)$  value is a crucial element that serves as the primary feature in the Langmuir isotherm model. The RL value serves as an indicator for the sort of adsorption taking place inside a specific system. A value of RL < 1 suggests the adsorption process that happens was strong; if RL > 1, it suggests to the adsorption process that occurs is weak; RL = 0 indicates that the adsorption process that occurs is irreversible; while 0 < RL < 1 suggests to the favorable adsorption. The RL value may be derived using the equation:

$$R_L = \frac{1}{1 + K_L C_e} \tag{5}$$

Based on the RL values obtained as presented in Table 1, it can be assumed from the fact that Cr(VI) adsorption procedure is resulting in a favorable direction. A favorable adsorption is one that has a convex shape in the adsorption isotherm, reflecting a substantial quantity of adsorption at a low liquid concentration.

## 3.4 Freundlich isotherm model

The model of Freundlich isotherm characterizes how the adsorption process occurring heterogeneously on surfaces during the contact with adsorbate molecules. This model elucidates the variability of the adsorbent surface, leading to disparities in energy across different adsorbent sites. [30]. The isotherm model for the Cr(VI) adsorption process by WC is illustrated in Figure 4.

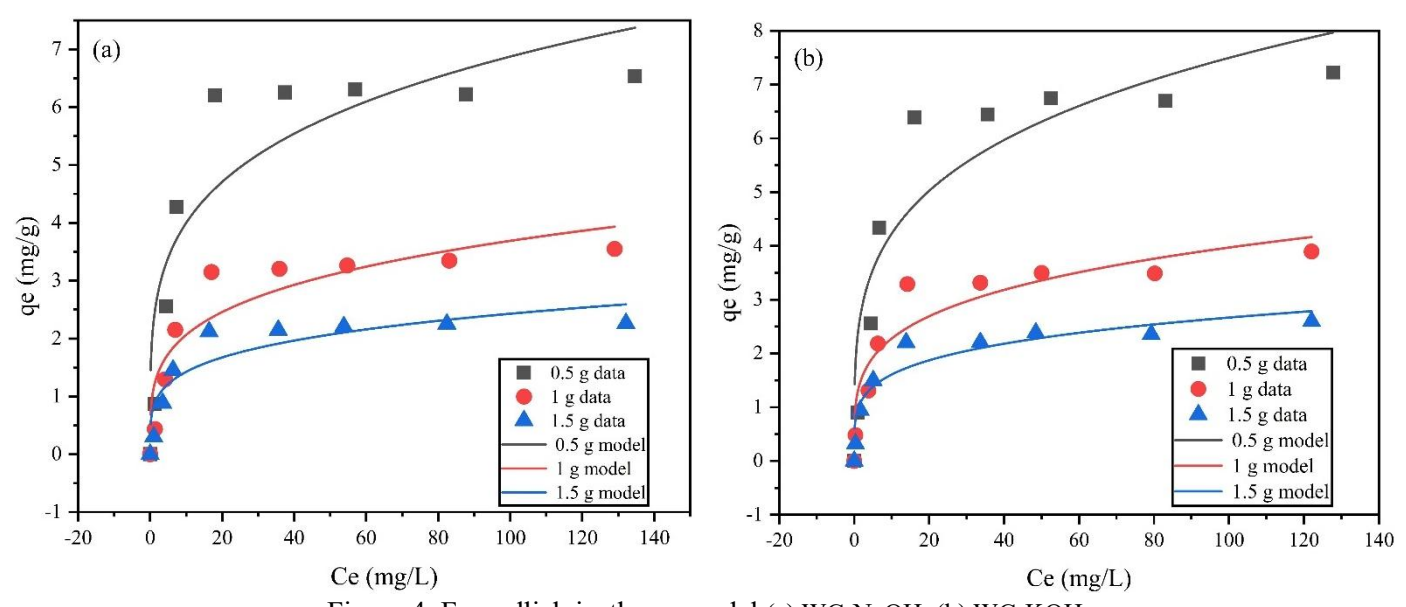


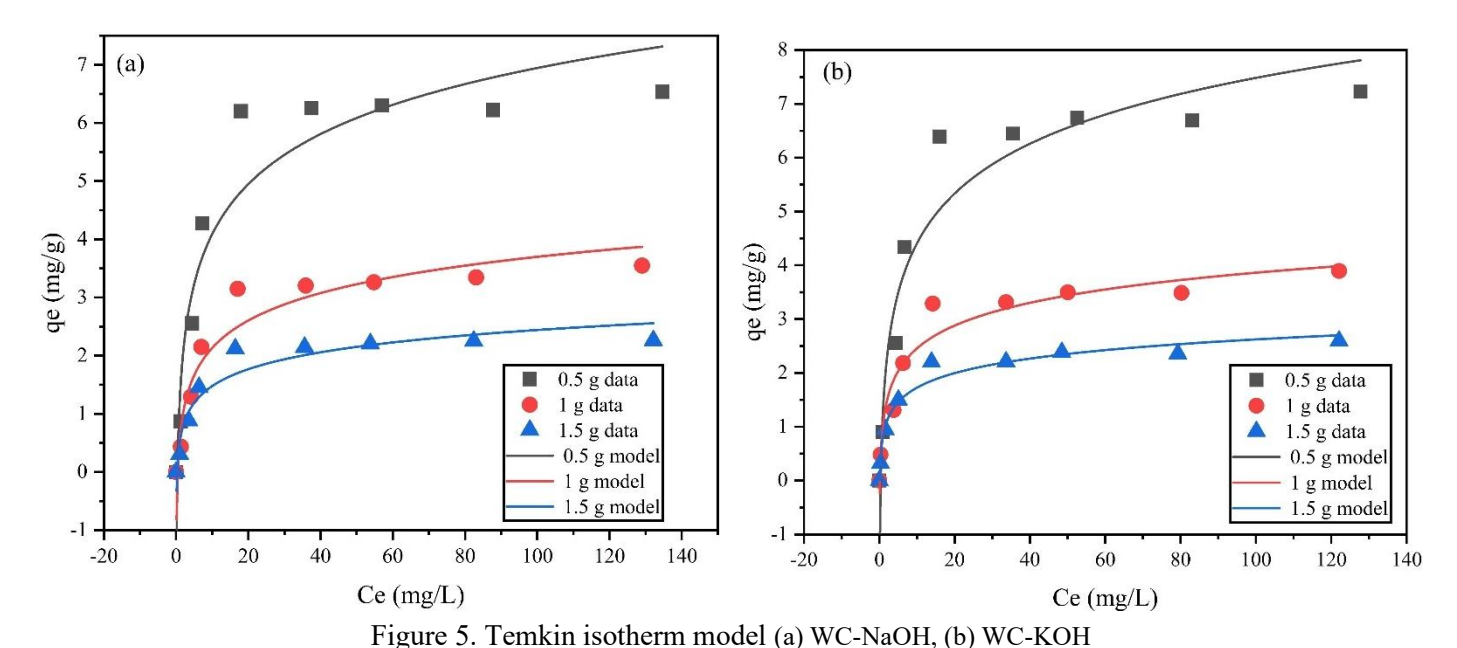
Figure 4. Freundlich isotherm model (a) WC-NaOH, (b) WC-KOH

The results indicate a reduction in the K<sub>F</sub> value simultaneous with a rise in the adsorbent quantity, as illustrated in Table 4. This transpires in both categories of adsorbents (WC-NaOH and WC-KOH). A lower adsorbent mass often results in a raised KF value, attributable to a rise of the qe value that come due to limiting of the sites of adsorption, which subsequently gets higher Ce. A greater adsorbent mass typically results in a diminished qe value, as the adsorbate is distributed over more active sites. So it can be stated that based on the results obtained, the bigger the K<sub>F</sub> value, the greater the adsorption power of the adsorbent. WC-KOH exhibits a superior K<sub>F</sub> value (2.3850 L/g) relative to WC-NaOH (2.3276 L/g), suggesting that, according to the Freundlich isotherm model, WC-KOH possesses enhanced adsorption capacity compared to WC-NaOH. In addition, one of several crucial variables associated with the Freundlich isotherm model is the 1/n value. Following the information received in Table 4, the Cr(VI) adsorption process that occurs in both types of adsorbents reveals a positive adsorption process. This can be seen from the 1/n value of both adsorbents, showing a value of 1<.

# 3.5 Temkin Isotherm Model

A Temkin equilibrium model was implemented for assessing the adsorption properties of Cr(VI) on the outer layers of WC-KOH or WC-NaOH adsorbents by considering the interaction impact between the adsorbate (Cr(VI)) and the adsorbent surface, as well as the variation of adsorption energy. The results of the charting with the Temkin isotherm model can be seen in Figure 5.

The outcomes summarized in Table 4 suggest that the WC-KOH and WC-NaOH adsorbents exhibit notable differences in their adsorption characteristics for Cr(VI), particularly regarding adsorption energy and affinity for Cr(VI) ions. WC-KOH exhibits a greater affinity constant value (A) compared to WC-NaOH, signifying its superior capacity to adsorb Cr(VI), particularly at elevated concentrations. The larger surface area and prevalence of micropores in WC-KOH contribute to an increased number of active sites for chemical binding. In contrast, WC-NaOH, characterized by a more pronounced mesoporous structure, exhibits a lower value of the adsorption energy parameter (B). This suggests a more homogeneous distribution of adsorption energy in WC-NaOH. However, its affinity for Cr(VI) is comparatively less than that of WC-KOH. The analysis of the Temkin isotherm model indicates that the coefficient A increases, whereas the corresponding value of B reduces with a rising in adsorbent mass for both materials, WC-KOH and WC-NaOH. The increase in the A value indicates that with enhancing adsorbent mass, the total quantity of active sites that can interact with ions from Cr(VI) also increases, so the adsorbent affinities for Cr(VI) become higher.



nificance of WC-KOH lies in its extensive surface area along with its abundan

The significance of WC-KOH lies in its extensive surface area along with its abundance of micropores, which facilitate greater accumulation of Cr(VI) and lead to a higher increase in affinity compared to WC-NaOH. The reduction in the B value indicates that the average adsorption energy per Cr(VI) molecule diminishes as the mass of the adsorbent increases. The reduction is attributed to diminished energy competition on the surface of the adsorbent as a larger amounts of active locations become accessible. In WC-NaOH, characterized by a predominant mesoporous structure, the reduction in adsorption of energy is more stable due to more homogeneous energy distribution. Meanwhile, in WC-KOH, which has a microporous structure, the decrease in B is sharper because adsorption at high energy sites (micropores) has occurred at an early stage, so that with the increase in adsorbent mass, sites with lower energy become more dominant.

## 3.6 Dubinin-Raduskevich Isotherm Model

Dubinin-Raduskevich (D-R) isotherm model effectively represents the adsorption processes on porous surfaces exhibiting heterogeneous adsorption energy [31]. The D-R model suggests that the micropores in the adsorbent dominate the adsorption process, compared to the Langmuir model. Figure 6 demonstrates the D-R Isotherm Model. The results indicate many parameters of the D-R isotherm model, including qm, KDR, and E, as detailed in Table 4. The qm value derived from the D-R isotherm model indicates that WC-KOH yields a higher qm value (6.8570 mg/g) than WC-NaOH (6.4052 mg/g). This value denotes the maximum quantity of Cr(VI) that the adsorbent can absorb. The parameters that significantly affect the D-R isotherm model are the KDR and E values. The KDR value correlates with the adsorption energy. Both parameters will be connected where a bigger KDR value will create a smaller E value. The KDR value achieved in WC-NaOH and WC-KOH will be reduced as the adsorbent mass increases. When the adsorbent mass grows, the quantity of active sites during the adsorption are going to increase. More active sites will result in Cr(VI) finding the adsorption site more easily by requiring lesser energy. The limitation of active sites accessible on a smaller adsorbent mass will result in competition between Cr(VI) to attach to sites that have higher energy. The E value generated on both adsorbents according to the D-R isotherm model shows that the Cr(VI) adsorption process occurs physically (E<8 KJ/mol) where the adsorption process that occurs is controlled by Van der Waals forces so that Cr(VI) only attaches to the surface of the adsorbent without any changes in chemical structure or significant ion exchange and its adsorption efficiency can be significantly affected by the particular amount of surface area and number of active spots.

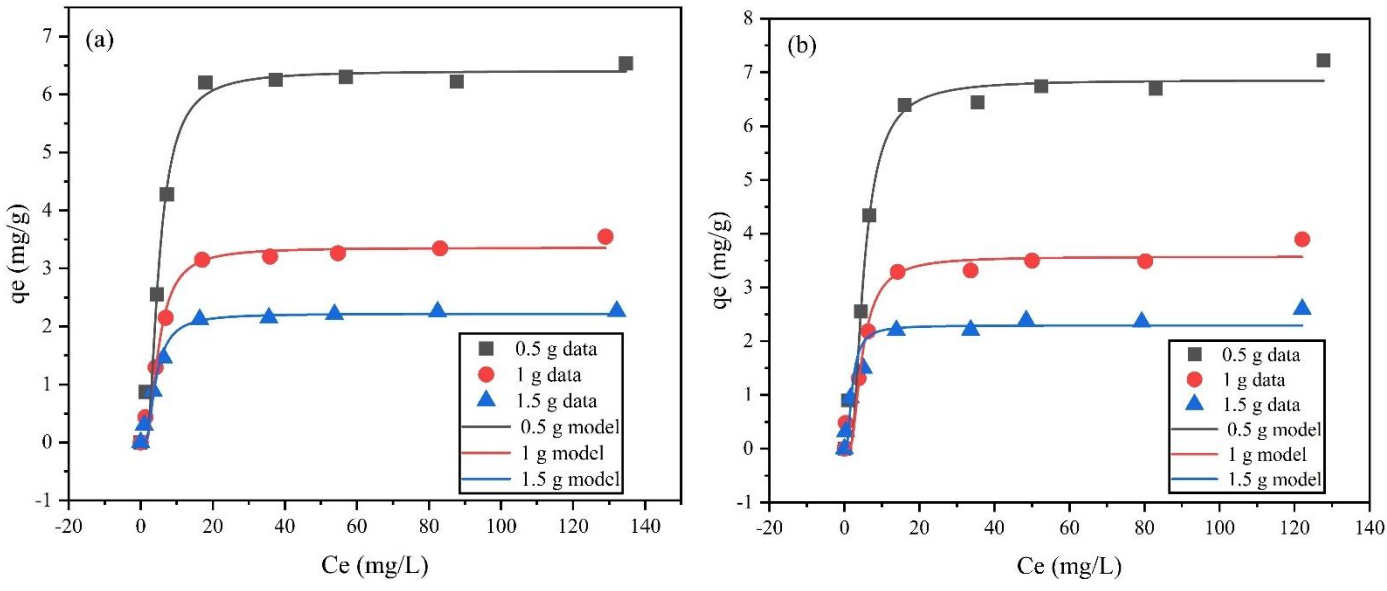


Figure 6. Dubinin-Raduskevich isotherm model (a) WC-NaOH, (b) WC-KOH

Table 3 indicates that most significantly appropriate isotherm model for interpreting the Cr(VI) adsorption process by NaOH-WC and KOH-WC adsorbents is, in order of preference, Langmuir > Dubinin-Raduskevich > Temkin > Freundlich. It can be observed from the values of the coefficient of correlation (R<sup>2</sup>), sum square error (SSE), and chi-square (x<sup>2</sup>), which are presented in Table 3. These statistical measurements provide a complete assessment of the model's performance and its capacity to explain the variability in the data. A detailed investigation of these numbers gives valuable insights about the relationship between the parameters under the study. Multiple models suggest that the WC-KOH adsorbent exhibits superior adsorption capacity relative to WC-NaOH, as reflected by the higher qmax value. The findings indicate that the adsorption process of Cr(VI) by NaOH-WC and KOH-WC is homogeneous, implying uniform energy across all adsorption sites. The adsorption process transpires on a single surface (monolayer), with no buildup on the adsorbent's surface. The Langmuir isotherm model suggests that there is no interaction between Cr(VI) on the surface of the adsorbent, and the step of adsorption is seen as reversible, with equilibrium established between the adsorbed Cr(VI) molecules and those in the solution. The activation procedure with KOH and NaOH will generate micropores and mesopores, hence increasing the number of accessible adsorption sites. Activation with potent bases (KOH or NaOH) generates functional oxygen groups, including hydroxyl (-OH) and carbonyl (-C=O), on the surface of wood charcoal. These groups may engage with Cr(VI) ions via the establishment of hydrogen bonds or alternative chemical interactions. Previous research by Saad, 2020 [32] confirms the production of (-OH), (C-H), and (-C=O) groups during activation with KOH and NaOH.

# 3.7 Adsorption Kinetics

Pseudo-first order (PFO) alongside pseudo-second-order (PSO) kinetic approaches have been employed for determining the parameters of the kinetics of Cr(VI) removal via WC-NaOH or WC-KOH. A PFO Kinetic Modeling implies how the Cr(VI) adsorption mechanism can occur owing to internal diffusion, and the rate of adsorption will be correlated to the total amount of active sites left present from the surface of the adsorbent. Meanwhile, a PSO kinetic model posits the idea that the adsorption kinetic rate will eventually be modulated by the chemical interaction throughout the adsorbate molecules and the particles of the adsorbent. The plotting results of the PFO and PSO kinetic models may be presented in Figure 7.

Table 3 Adsorption Isotherm Model Constant for Cr(VI) removal by WC-NaOH and WC-KOH

| Isotherm Model            | WC-NaOH |        |        | WC-KOH |        |        |
|---------------------------|---------|--------|--------|--------|--------|--------|
| Constant                  | 0.5 g   | 1 g    | 1.5 g  | 0.5 g  | 1 g    | 1.5 g  |
| Langmuir:                 |         |        |        |        |        |        |
| qmax (mg/g)               | 7.0085  | 3.7271 | 2.4293 | 7.5460 | 3.9317 | 2.5253 |
| $K_L \left( L/mg \right)$ | 0.1806  | 0.1691 | 0.2107 | 0.1738 | 0.1907 | 0.3444 |

IPTEK, The Journal of Engineering, Vol. 11, No. 2, 2025 (eISSN: 2807-5064)

| $R_{\rm L}$                        | 0.0395-0.8111 | 0.0438-0.8210 | 0.0347-0.8296 | 0.0431-0.8551         | 0.0412-0.9381      | 0.0232-0.8936 |
|------------------------------------|---------------|---------------|---------------|-----------------------|--------------------|---------------|
| $\mathbb{R}^2$                     | 0.9714        | 0.9796        | 0.9840        | 0.9758                | 0.9751             | 0.9912        |
| SSE                                | 1.5293        | 0.3037        | 0.1044        | 1.4898                | 0.4210             | 0.0664        |
| $x^2$                              | 0.4428        | 0.1877        | 0.0888        | 0.3615                | 0.3876             | 0.0417        |
| Freundlich:                        |               |               |               |                       |                    |               |
| $K_F(L/g)$                         | 2.3276        | 1.1552        | 0.8372        | 2.3850                | 1.3068             | 0.9704        |
| 1/n                                | 0.2352        | 0.2521        | 0.2313        | 0.2487                | 0.2413             | 0.2196        |
| n                                  | 4.2517        | 3.9667        | 4.3234        | 4.0209                | 4.1442             | 4.5537        |
| $\mathbb{R}^2$                     | 0.7611        | 0.8064        | 0.7922        | 0.8097                | 0.8630             | 0.8817        |
| SSE                                | 7.6557        | 1.7690        | 0.8186        | 7.2101                | 1.4426             | 0.5470        |
| $\mathbf{x}^2$                     | 2.1125        | 0.9872        | 0.6600        | 1.9651                | 0.7548             | 0.4518        |
| Temkin:                            |               |               |               |                       |                    |               |
| A(L/g)                             | 2.7137        | 2.3130        | 3.4401        | 2.7175                | 5.5887             | 8.4545        |
| B (KJ/mol)                         | 1.2395        | 0.6796        | 0.4181        | 1.3351                | 0.6106             | 0.3892        |
| $\mathbb{R}^2$                     | 0.9213        | 0.9434        | 0.9382        | 0.9422                | 0.9537             | 0.9760        |
| SSE                                | 4.2037        | 0.8451        | 0.4030        | 3.5597                | 0.7844             | 0.1811        |
| $\mathbf{x}^2$                     | 1.0574        | 0.4273        | 0.2897        | 0.8242                | 0.3492             | 0.1105        |
| Dubinin-                           |               |               |               |                       |                    |               |
| Raduskevich:                       |               |               |               |                       |                    |               |
| qmax (mg/g)                        | 6.4052        | 3.3569        | 2.2196        | 6.8570                | 3.5716             | 2.2937        |
| $K_{DR} \left( mol^2/KJ^2 \right)$ | 22.6283       | 21.5570       | 15.9035       | 23.5805               | 19.9760            | 4.6033        |
| E (KJ/mol)                         | 0.1487        | 0.1523        | 0.1773        | 0.1456                | 0.1582             | 0.3296        |
| $\mathbb{R}^2$                     | 0.9838        | 0.9824        | 0.9823        | 0.9825                | 0.9753             | 0.9374        |
| SSE                                | 0.8651        | 0.2624        | 0.1157        | 1.0766                | 0.4181             | 0.4723        |
| $\mathbf{x}^2$                     | 203.8205      | 68.0560       | 112.2202      | $15.0903 \times 10^3$ | $6.72 \times 10^4$ | 220.342       |

The investigation indicates that the PSO kinetic model yields a superior model fit relative to the PFO kinetic model. The models we value correspond precisely with the experimental value, as evidenced by the R², SSE, and x² criteria. The PSO kinetic model obtained an R² value close to 1 and smaller SSE and x² values when compared with the PFO model. indicates that the PSO model not only provides a better fit to the data but also suggests a more accurate representation of the underlying processes at play. Consequently, these findings support the preference for the PSO Kinetic Model in future analyses and applications. The concentration of the adsorbate influences the kinetic parameters, specifically qe and k2, according to the PSO kinetic approach, as illustrated within Table 4.

The qe value generally rises with an upward trend in initial Cr(VI) amount. This transpires as a larger concentration of Cr(VI) results in an increased availability of ions of Cr(VI) for adsorption onto the active sites of the adsorbent surface. When the initial concentration increases, the potential for a bigger concentration gradient causes the diffusion regarding Cr(VI) ions from the solution to the adsorbent surface, hence increasing the amount of Cr(VI) ions adsorbed until equilibrium is attained. The k2 value, indicative of the adsorption rate constant according to the PSO kinetic model, demonstrates an inverse relationship, as it diminishes with rising Cr(VI) concentration. This suggests that at elevated concentrations, the duration to achieve adsorption equilibrium increases as the majority of active sites get occupied, leading to in a deceleration from the chemical reaction rate across Cr(VI) ions and the adsorption medium. Furthermore, a saturation of active sites at elevated concentrations can diminish the effectiveness of the kinetic process. The adsorbents WC-KOH and WC-NaOH exhibit notable disparities in pseudo-second-order (PSO) kinetic characteristics. WC-KOH adsorbents often exhibit superior equilibrium adsorption capacity (ge) compared to WC-NaOH. Since KOH facilitates the development of a larger surface area, an increased quantity of micropores, and a more efficient pore distribution, hence enhancing the abundance regarding active sites for Cr(VI) adsorption. In contrast, WC-NaOH generally shows a larger kinetic rate constant (k2) because modification with NaOH provides additional functional substances including hydroxyl (-OH) and carbonyl (C=O), thereby increasing the chemisorption interaction. Although WC-KOH is greater in adsorption capacity, its k2 value is lower because the dominance of micropores can

slow down the transport of ions containing Cr(VI) to the places of action. In addition, WC-KOH is more structurally stable after multiple regeneration cycles, making it more suitable for long-term applications, whereas WC-NaOH is more effective for operations with shorter contact times. The mechanism of adsorption for Cr(VI) based on the PSO kinetic model on WC-KOH and WC-NaOH adsorbents shows that this process is controlled by chemisorption, including the generation of powerful chemical interactions among Cr(VI) ions and functional groups on the surface of the adsorbent, involving hydroxyl (-OH) and carbonyl (C=O). The existence of these functional groups on the surface of the adsorbent can be confirmed based on several previous studies that have been carried out by Saad et al, [32], Demiral et al [33], Mladenović Nikolić et al[34] and Jiao et al[35]. The huge specific surface area and number of micropores in WC-KOH make it possible for a larger equilibrium adsorption capacity (qe). This happens since there are more active sites that can bind Cr(VI) ions. On the other hand, WC-NaOH, which has a more dominating mesoporous structure, produces a higher kinetic rate (k2) considering its diffusion of Cr(VI) ions to the surface of the adsorbent is faster, initial concentration variation of Cr(VI) also affects the adsorption process. A higher concentration allows quicker for the ions of Cr(VI) to transfer to the adsorbent surface until the concentration gradient approaches equilibrium. A study that looks at both diffusion through pores and chemisorption finds that WC-KOH has a higher adsorption capacity because it contains more micropores, but WC-NaOH has a faster kinetic rate because active sites can be reached through mesopores. This can be validated through various previous investigations undertaken by Tseng et al, Cazetta et al, Jawad et al, and Hafizuddin et al [36], [37], [38], [39] which states the presence of KOH activator will generate more micropores (<2 nm), resulting in a higher adsorption capacity due to the redox reaction between the KOH and the material contributes to the formation of a dense pore structure compared to the NaOH activator, which typically creates mesopores (2–50 nm) due to a more aggressive the etching process on the carbon structure, allowing a quicker adsorption rate since it facilitates the diffusion of molecules to the active site and generate faster adsorption kinetics despite the total adsorption capacity is lower.

In addition, the findings from the current investigation indicate that the results of isotherm modeling utilizing the D-R equation reveal an E value of less than 8 KJ/mol. This suggests that the adsorption process is characterized by physisorption. On the other hand, the adsorption kinetics data, which align with the PSO kinetic model, suggest that the process is associated with chemisorption. The simultaneous occurrence of two mechanisms can lead to this phenomenon. In various adsorption systems, particularly those utilizing heterogeneous adsorbents like wood charcoal activated with alkali compounds, both physical and chemical adsorption may take place concurrently. This combination facilitates adsorption through multiple mechanistic pathways. Chemical adsorption can take place on the functional groups present on the adsorbent surface, whereas physical adsorption is observed within larger microscopic pores. The low adsorption energy is represented in the isotherm model, whereas the kinetic process remains governed by the chemical mechanism occurring on the active surface.

Table 4 Kinetics Model Parameters for Cr(VI) removal onto WC-NaOH and WC-KOH

| Kinetics<br>Model<br>Constant       | WC-NaOH |         |         | WC-KOH  |         |         |  |
|-------------------------------------|---------|---------|---------|---------|---------|---------|--|
|                                     | 10 mg/L | 30 mg/L | 50 mg/L | 10 mg/L | 30 mg/L | 50 mg/L |  |
| PFO:                                |         |         |         |         |         |         |  |
| qe (mg/g)                           | 0.7811  | 2.3662  | 3.2730  | 0.8544  | 2.4254  | 3.4001  |  |
| k <sub>1</sub> (min <sup>-1</sup> ) | 0.1136  | 0.1187  | 0.1002  | 0.0943  | 0.1244  | 0.1041  |  |
| $\mathbb{R}^2$                      | 0.9825  | 0.9868  | 0.9902  | 0.9828  | 0.9952  | 0.9941  |  |
| SSE                                 | 0.0091  | 0.0625  | 0.0878  | 0.0105  | 0.0236  | 0.0567  |  |
| $x^2$                               | 0.0117  | 0.0265  | 0.0272  | 0.0125  | 0.0098  | 0.0168  |  |
| PSO:                                |         |         |         |         |         |         |  |
| qe (mg/g)                           | 0.8276  | 2.4915  | 3.4788  | 0.9175  | 2.5238  | 3.5898  |  |
| k <sub>2</sub> (g/mg.min)           | 0.2972  | 0.1114  | 0.0619  | 0.1991  | 0.1395  | 0.0674  |  |
| $\mathbb{R}^2$                      | 0.9907  | 0.9935  | 0.9967  | 0.9923  | 0.9984  | 0.9985  |  |
| SSE                                 | 0.0048  | 0.0310  | 0.0297  | 0.0047  | 0.0078  | 0.0145  |  |
| $\mathbf{x}^2$                      | 0.0063  | 0.0135  | 0.0094  | 0.0056  | 0.0033  | 0.0044  |  |

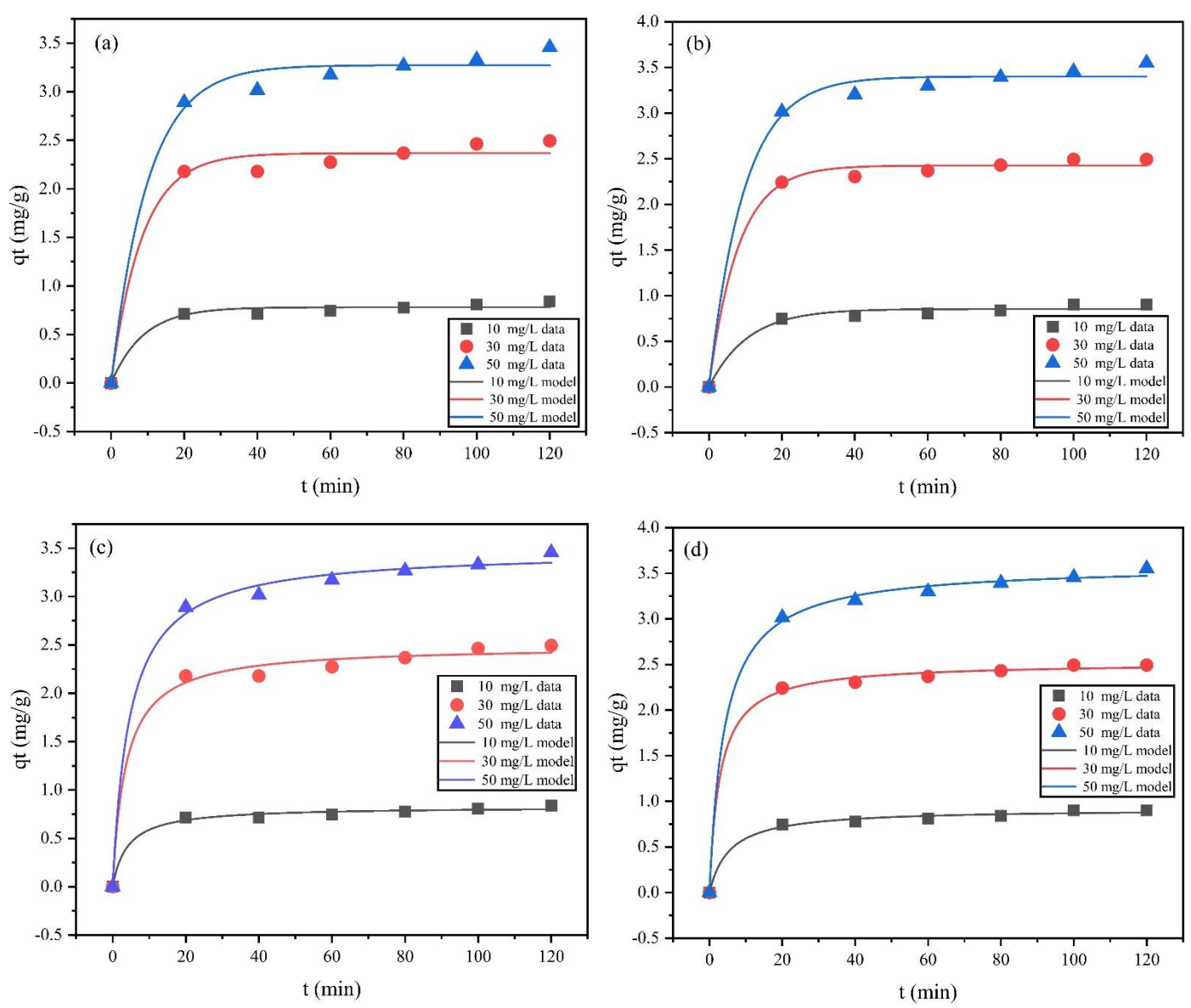


Figure 7. PFO kinetic models (a) WC-NaOH; (b) WC-KOH and PSO kinetic models; (c) WC-NaOH; (d) WC-KOH 3.8 Desorption and Regeneration Study

Following the procedure of adsorption, it becomes fundamental to perform both desorption and regeneration procedures on the WC-NaOH and WC-KOH adsorbents. The primary objective of the desorption and regeneration process of adsorbent to reinstate the capacity for adsorption of the material that has become saturated with pollutants, enabling its reuse in subsequent adsorption cycles. This method seeks to eliminate pollutants adsorbed on the material's surface (by desorption) and to restore the physicochemical qualities of the adsorbent, ensuring its continued efficacy in binding contaminants. Regeneration enhances operational cost efficiency by decreasing the necessity for new materials and promoting environmental sustainability through the reduction of spent adsorbent waste. This procedure facilitates the safe management of toxic waste, ensuring that adsorption technology may be used both cheaply and sustainably over the long term. The desorption and regeneration of the WC-NaOH and WC-KOH adsorbents are executed by introducing the used adsorbent into a mixture of ethanol and 0.1 M NaOH, following a modified version of the established approach by [27]. The findings gained have been shown in Figure 8.

Regarding the results presented in Figure 6, there is an overall decrease in efficiency for WC-NaOH and WC-KOH regarding Cr(VI) adsorption from cycles 1 to 4. The reduction in efficiency may be attributed to various factors, including Throughout the regeneration cycle, the adsorbent may undergo morphological alterations, including pore degradation or a reduction in the amount of surface area. This minimizes the quantity of active surface area accessible for the adsorption for Cr(VI). Moreover, the active locations on the surface of the adsorbent may be diminished or altered during regeneration, adsorbent particles may aggregate during this process, consequently limiting contaminant

accessibility to the active surface. Additionally, certain Cr(VI) ions may become irreversibly attached to the adsorbent during the initial cycle, rendering them challenging to release via the desorption solution. This diminishes the adsorption capability for the subsequent cycle. The findings of the regeneration study indicate that WC-NaOH and WC-KOH adsorbents are effective in eliminating Cr(VI) contamination. So, further investigation, such as post-reaction surface characterization using FTIR, SEM, or BET, is highly recommended to understand the mechanism of efficiency decrease and the possibilities for adsorbent modification to improve regeneration stability and can be applied in upcoming studies.

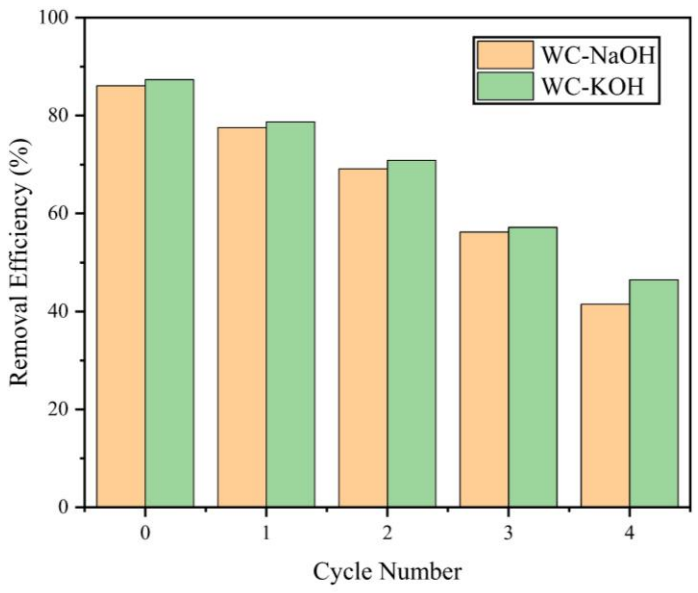


Figure 6. Regeneration performnace of WC-NaOH and WC-KOH for Cr(VI) removal

Based on comparative study data of WC-NaOH and WC-KOH adsorbents, the adsorption capacity values obtained tend to be near to numerous prior studies so that both adsorbents have very good potential. In addition, prior research demonstrated the fact that the Cr(VI) adsorption phases has been dominated by the Langmuir isotherm framework and the kinetic approach which correlates with PSO. The chemical adsorption of Cr(VI) on alkali-treated wood charcoal happens uniformly, with all adsorption sites possessing identical energy, resulting in a monolayer formation devoid of interactions among adsorbate molecules. The maximum adsorption capacity (qmax) is constrained, signifying that the adsorbent possesses a definitive threshold for binding Cr(VI), but the Langmuir constant (KL) reflects a robust affinity for both the absorbent alongside an adsorbate. In response to the PSO approach, the procedure for adsorption can be controlled by chemisorption, a chemical process that entails the transfer or sharing of electrons between Cr(VI) and the adsorbent, signifying that this process is significantly affected by the chemical properties of the material. The kinetic parameters (k2) and equilibrium capacity (qe) of the PSO model that are in good accordance alongside the findings from experiments show the accuracy of this model in capturing the dynamics of adsorption. With these data, it can be inferred that this adsorbent is particularly efficient in extracting Cr(VI) from wastewater and has significant potential for practical applications in environmental treatment. Moreover, as shown by several previous studies on the Cr(VI) removal approach highlighted in Table 6, the WC-NaOH and WC-KOH adsorbents showed significant potential, exhibiting relative high adsorption capacity values compared with several other types of adsorbents.

With a relatively similar adsorption capacity to other types of adsorbents and abundant availability of raw materials, this kind of adsorbent has the potential to be implemented in real-scale applications, especially in the treatment of industrial wastewater containing heavy metals, such as in the leather tanning industry, electroplating, and battery waste processing. To improve its relevance and effectiveness in actual situations, further investigations will be required focusing on the scale of application, the durability of the adsorbent in long-term regeneration cycles, and its effectiveness under multi-contaminant circumstances. In addition, this adsorbent can be integrated into a continuous filtration system or flow column for small- to medium-scale wastewater treatment. Therefore, the results of this work

can give real contributions in creating inexpensive, ecologically acceptable, and efficient adsorption methods to combat heavy metal pollution, notably Cr(VI), in aquatic environments.

Table 6. Comparison of Several Adsorbent in Cr(VI) removal

| Adsorbent                                 | qmax(mg/g) | Isotherm and Kinetics Models | References |
|---|------------|------------------------------|------------|
| Activated carbon supported iron catalysts | 26.97      | Langmuir, PFO                | [40]       |
| Banana Peel                               | 10.42      | Langmuir, PSO                | [41]       |
| Corn Stark Biochar                        | 17.07      | Freundlich, PSO              | [42]       |
| Single-walled Carbon<br>Nanotubes         | 2.35       | Langmuir, PSO                | [13]       |
| Chitosan/bentonite composite              | 16.38      | Redlich-Peterson, Elovich    | [43]       |
| Functionalized cellulose                  | 55         | Langmuir, PSO                | [40]       |
| WC-KOH                                    | 7.5460     | Langmuir, PSO                | This Work  |
| WC-NaOH                                   | 7.0085     | Langmuir, PSO                | This Work  |

#### 4. Conclusion

The present study revealed that chemically treated WC-KOH and WC-NaOH adsorbents were highly successful in removing the ions of Cr(VI) from aqueous solution via the mechanisms defined by the Langmuir isotherm framework and the PSO kinetic model. The outcomes suggested that the Langmuir isotherm model was the best acceptable model, with characteristics illustrating that adsorption developed as a monolayer on a homogeneous adsorbent surface. WC-KOH adsorbent showed a higher maximum adsorption capacity (qmax) than WC-NaOH, indicating its better capacity to remove Cr(VI), which was corroborated by its bigger specific surface area and number of micropores. In addition, the larger Langmuir constant (KL) value of WC-KOH claimed a better affinity for Cr(VI) ions. The PSO kinetic model was also demonstrated to be the best approach to represent the adsorption rate of Cr(VI) on both adsorbents. The model indicates the adsorption procedure is dominated because of chemisorption, with the reaction rate depending on the number of active sites accessible on the adsorbent surface. The WC-NaOH adsorbent, however having a lower adsorption capacity, demonstrated a higher kinetic rate constant (k2), demonstrating its ability to rapidly absorb Cr(VI) at the first stage of adsorption. Analytical methods using the non-linear Langmuir isotherm model and PSO kinetics offered more accurate results compared to the linear method, reducing systematic mistakes that sometimes occur in data processing. With this combination, the investigation found that WC-KOH is superior for applications needing strong adsorption capacity at high Cr(VI) concentrations, whereas WC-NaOH is more suitable for procedures with shorter contact durations at low to moderate concentrations. These insights give essential information over the establishment of modified biomass-based adsorption approaches to processing of hazardous wastes.

# Acknowledgments

Our team is pleased to express our profound gratitude to Politeknik Industri Logam Morowali for technical support for this research. A particular thanks to partners for their tremendous assistance and enlightening talks throughout the research process. This project was made possible via the collaboration and assistance of everybody concerned

#### References

- [1] J. P. Castro *et al.*, "Massaranduba sawdust: A potential source of charcoal and activated carbon," *Polymers* (*Basel*)., vol. 11, no. 8, pp. 1–14, 2019,
- [2] X. Wang, Z. Guo, Z. Hu, and J. Zhang, "Recent advances in biochar application for water and wastewater treatment: A review," *PeerJ*, vol. 8, 2020,
- [3] A. Chandrasekaran, S. Subbiah, P. Bartocci, H. Yang, and F. Fantozzi, "Carbonization using an Improved Natural Draft Retort Reactor in India: Comparison between the performance of two woody biomasses, Prosopis juliflora and Casuarina equisetifolia," *Fuel*, vol. 285, p. 119095, 2021,
- [4] G. Enaime, A. Baçaoui, A. Yaacoubi, and M. Lübken, "Biochar for Wastewater Treatment—Conversion Technologies and Applications," 2020.
- [5] N. Chaukura, T. M. Masilompane, W. Gwenzi, and A. K. Mishra, "Biochar-Based Adsorbents for the Removal of Organic Pollutants from Aqueous Systems," in *Emerging Carbon-Based Nanocomposites for Environmental Applications*, 2020, pp. 147–174.
- [6] W. Gwenzi, N. Chaukura, C. Noubactep, and F. N. D. Mukome, "Biochar-based water treatment systems as a potential low-cost and sustainable technology for clean water provision," *J. Environ. Manage.*, vol. 197, pp. 732–749, 2017,
- [7] T. K. Das and A. Poater, "Review on the use of heavy metal deposits from water treatmentwaste towards catalytic chemical syntheses," *Int. J. Mol. Sci.*, vol. 22, no. 24, 2021,
- [8] L. Cervera-Gabalda and C. Gómez-Polo, "Magnetic Fe/Fe3C@C Nanoadsorbents for Efficient Cr (VI) Removal," 2022.
- [9] H. Haeril, F. D. I. Sawali, and M. A. Afandy, "Phytoremediation of Cr(VI) from Aqueos Solution by Pistia stratiotes L.: Efficiency and Kinetic Models," *J. Tek. Kim. dan Lingkung.*, vol. 8, no. 1, pp. 25–35, 2024,
- [10] D. Mahringer, S. S. Zerelli, U. Dippon, and A. S. Ruhl, "Pilot scale hexavalent chromium removal with reduction, coagulation, filtration and biological iron oxidation," *Sep. Purif. Technol.*, vol. 253, no. June, p. 117478, 2020,
- [11] M. L. Rahman *et al.*, "Poly(hydroxamic acid) ligand from palm-based waste materials for removal of heavy metals from electroplating wastewater," *J. Appl. Polym. Sci.*, vol. 138, no. 2, pp. 1–16, 2021,
- [12] K. K. Onchoke and S. A. Sasu, "Determination of Hexavalent Chromium (Cr(VI)) Concentrations via Ion Chromatography and UV-Vis Spectrophotometry in Samples Collected from Nacogdoches Wastewater Treatment Plant, East Texas (USA)," *Adv. Environ. Chem.*, vol. 2016, no. Iii, pp. 1–10, 2016,
- [13] M. E. Mahmoud, M. F. Amira, S. M. Seleim, and A. K. Mohamed, "Amino-decorated magnetic metal-organic framework as a potential novel platform for selective removal of chromium (VI), cadmium (II) and lead (II)," *J. Hazard. Mater.*, vol. 381, no. Vl, p. 120979, 2020,
- [14] J. Bayuo, "An extensive review on chromium (vi) removal using natural and agricultural wastes materials as alternative biosorbents," *J. Environ. Heal. Sci. Eng.*, vol. 19, no. 1, pp. 1193–1207, 2021,
- [15] V. Yogeshwaran and A. K. Priya, "Removal of Hexavalent Chromium (Cr6+) Using Different Natural Adsorbents A Review," *J. Chromatogr. Sep. Tech.*, vol. 08, no. 06, pp. 1–20, 2016,
- [16] A. Khandelwal, N. Narayanan, E. Varghese, and S. Gupta, "Linear and Nonlinear Isotherm Models and Error Analysis for the Sorption of Kresoxim-Methyl in Agricultural Soils of India," *Bull. Environ. Contam. Toxicol.*, vol. 104, no. 4, pp. 503–510, 2020,
- [17] R. Sahin and K. Tapadia, "Comparison of linear and non-linear models for the adsorption of fluoride onto geomaterial: Limonite," *Water Sci. Technol.*, vol. 72, no. 12, pp. 2262–2269, 2015,
- [18] Markandeya, S. P. Shukla, and G. C. Kisku, "Linear and non-linear kinetic modeling for adsorption of disperse dye in batch process," *Res. J. Environ. Toxicol.*, vol. 9, no. 6, pp. 320–331, 2015,

- [19] I. Umar, N. Bala, N. Danlami, and A. Y. Abdulfatah, "Comparison of Linear and Non-Linear Methods of Freundlich and Langmuir Isotherm Models for the Adsorption of Lead Using Sugarcane Bagasse," *Noble Int. J. Sci. Res.*, vol. 1, no. 5, pp. 69–72, 2017, [Online]. Available: http://napublisher.org/?ic=journals&id=2
- [20] J. Serafin and B. Dziejarski, "Application of isotherms models and error functions in activated carbon CO2 sorption processes," *Microporous Mesoporous Mater.*, vol. 354, no. March, 2023,
- [21] M. Shafiq, A. A. Alazba, and M. T. Amin, "Kinetic and isotherm studies of ni2+and pb2+adsorption from synthetic wastewater using eucalyptus camdulensis—derived biochar," *Sustain.*, vol. 13, no. 7, 2021,
- [22] T. M. Ting, M. M. Nasef, and K. Hashim, "Linear and non-linear regression analysis of boron adsorption kinetics on new radiation grafted fibrous adsorbent," *Appl. Mech. Mater.*, vol. 625, pp. 245–248, 2014,
- [23] N. Ayawei, A. N. Ebelegi, and D. Wankasi, "Modelling and Interpretation of Adsorption Isotherms," *J. Chem.*, vol. 2017, 2017,
- [24] F. Wahid, I. U. Mohammadzai, A. Khan, Z. Shah, W. Hassan, and N. Ali, "Removal of toxic metals with activated carbon prepared from Salvadora persica," *Arab. J. Chem.*, vol. 10, pp. S2205–S2212, 2017,
- [25] M. S. Fadila, M. A. Afandy, S. Suhirman, and M. I. Al Fuady, "Studi Kinetika dan Penentuan Dosis Optimum Koagulan FeCl3 dalam Menurunkan Konsentrasi Cu2+ pada Larutan," *React. J. Res. Chem. Eng.*, vol. 4, no. 2, pp. 60–67, 2023.
- [26] R. Saha, K. Mukherjee, I. Saha, A. Ghosh, S. K. Ghosh, and B. Saha, "Removal of hexavalent chromium from water by adsorption on mosambi (Citrus limetta) peel," *Res. Chem. Intermed.*, vol. 39, no. 5, pp. 2245–2257, 2013,
- [27] J. Qu *et al.*, "KOH-activated porous biochar with high specific surface area for adsorptive removal of chromium (VI) and naphthalene from water: Affecting factors, mechanisms and reusability exploration," *J. Hazard. Mater.*, vol. 401, no. June, p. 123292, 2021,
- [28] C. H. Chia, S. Zakaria, M. S. Sajab, and M. J. Saad, "Activated Carbon Produced from Rice Husk by NaOH and KOH Activation and its Adsorption in Methylene Blue," *Adv. Agric. Food Res. J.*, pp. 1–13, 2022,
- [29] Y. Guo, K. Yu, Z. Wang, and H. Xu, "Effects of activation conditions on preparation of porous carbon from rice husk [1]," *Carbon N. Y.*, vol. 41, no. 8, pp. 1645–1648, 2003,
- [30] M. A. Afandy and F. D. I. Sawali, "Adsorption of Chromium Hexavalent in Aqueous Solutions Using Acid-Activated Wood Charcoal: Isotherm and Kinetics Study," *J. Ilm. Tek. Kim.*, vol. 8, no. 1, pp. 1–14, 2024.
- [31] M. Musah, Y. Azeh, J. Mathew, M. Umar, Z. Abdulhamid, and A. Muhammad, "Adsorption Kinetics and Isotherm Models: A Review," *Caliphate J. Sci. Technol.*, vol. 4, no. 1, pp. 20–26, 2022,
- [32] M. J. Saad *et al.*, "Comparative adsorption mechanism of rice straw activated carbon activated with NaOH and KOH," *Sains Malaysiana*, vol. 49, no. 11, pp. 2721–2734, 2020,
- [33] İ. Demiral, C. Samdan, and H. Demiral, "Enrichment of the surface functional groups of activated carbon by modification method," *Surfaces and Interfaces*, vol. 22, p. 100873, 2021,
- [34] N. N. Mladenović Nikolić *et al.*, "Radiological and Structural Characterization of Raw and Alkali-Activated Wood Ash and Metakaolin Blends," 2022.
- [35] H. Jiao *et al.*, "Structure-property-function relationships of wood-based activated carbon in energy and environment materials," *Sep. Purif. Technol.*, vol. 353, p. 128607, 2025,
- [36] R.-L. Tseng and S.-K. Tseng, "Pore structure and adsorption performance of the KOH-activated carbons prepared from corncob," *J. Colloid Interface Sci.*, vol. 287, no. 2, pp. 428–437, 2005,
- [37] M. S. Hafizuddin, C. L. Lee, K. L. Chin, P. S. H'ng, P. S. Khoo, and U. Rashid, "Fabrication of Highly Microporous Structure Activated Carbon via Surface Modification with Sodium Hydroxide," 2021.
- [38] A. L. Cazetta *et al.*, "NaOH-activated carbon of high surface area produced from coconut shell: Kinetics and equilibrium studies from the methylene blue adsorption," *Chem. Eng. J.*, vol. 174, no. 1, pp. 117–125, 2011,

- [39] A. H. Jawad *et al.*, "Microporous activated carbon developed from KOH activated biomass waste: surface mechanistic study of methylene blue dye adsorption," *Water Sci. Technol.*, vol. 84, no. 8, pp. 1858–1872, Sep. 2021,
- [40] S. Rawat *et al.*, "Remediation of Cr(VI) using a radiation functionalized green adsorbent: Adsorption modelling, mechanistic insights and prototype water purifier demonstration," *J. Water Process Eng.*, vol. 60, p. 105109, 2024,
- [41] Ş. Parlayici and E. Pehlivan, "Comparative study of Cr(VI) removal by bio-waste adsorbents: equilibrium, kinetics, and thermodynamic," *J. Anal. Sci. Technol.*, vol. 10, no. 1, 2019,
- [42] X. Guo *et al.*, "Adsorption mechanism of hexavalent chromium on biochar: Kinetic, thermodynamic, and characterization studies," *ACS Omega*, vol. 5, no. 42, pp. 27323–27331, 2020,
- [43] J. Yang, B. Huang, and M. Lin, "Adsorption of Hexavalent Chromium from Aqueous Solution by a Chitosan/Bentonite Composite: Isotherm, Kinetics, and Thermodynamics Studies," *J. Chem. Eng. Data*, vol. 65, no. 5, pp. 2751–2763, 2020,